OPEN

NPG Asia Materials (2017) 9, e417; doi:10.1038/am.2017.139
www.nature.com/am

ORIGINAL ARTICLE

Hygromorphic actuator from a metal oxide film driven by a nano-capillary forest structure

Hosung Kang[1], Minki Lee[1], Hyuneui Lim[2], Howard A Stone[3] and Jinkee Lee[1]

We have developed a hygromorphic metal oxide actuator using an electrochemical method to produce a superhydrophilic free-standing nano-capillary forest of titanium oxide with a high aspect ratio (~80). This metal oxide film has an inhomogeneous initial gap at the top and bottom surfaces between the tubes due to flexure during fabrication. The actuation mechanism is as follows. First, when a drop of water is applied on the surface of a titanium oxide nano-capillary forest (TNF), the water penetrates through the film instantaneously, and the titanium oxide nano-capillaries are pulled together by interplay of the capillary force and van der Waals force. When water has fully filled in the gaps between the capillaries, the free-standing TNF film remains unbent for ~ 2 min. Then, as the water evaporates, the film bends further in the forward direction. When the water has completely evaporated, the van der Waals force alone acts on the capillaries, and the TNF film returns to its initial state. This TNF possesses great stability and repeatability for long-term usage having a high bending energy density of ~ 1250 kJ m^{-3} and unique capabilities. It may lead to novel stimuli-responsive systems, including energy collection and storage, as well as robotics applications.

NPG Asia Materials (2017) **9,** e417; doi:10.1038/am.2017.139; published online 4 August 2017

INTRODUCTION

Among the mechanical systems desired for many engineering applications, highly sensitive actuating devices are important.[1] Reversible and controlled two- or three-dimensional shape changes in response to external stimuli are the key characteristics of actuating devices such as cantilever sensors, artificial muscles, and even micro-robotics using smart materials and structures.[1–7] These types of actuators may respond to external stimuli such as humidity, temperature, electric fields, light, solvent composition or pH.[2–4,8–12] Recently, polymeric actuators that produce a rapid mechanical motion in an efficient way have been developed.[1] Nevertheless, non-polymeric actuators, except shape memory alloys, remain challenging to deform using external stimuli.

Various arrangements of material structures of many lengths work in concert to perform diverse mechanical functions. For example, hygromorphic structures in nature, such as the passive movement of pinecones or wheat awn and the dispersal and self-burial of seeds, accomplish vital tasks for an organism's survival.[13–15] These hygromorphic structures can possibly exhibit high energy densities and therefore can potentially play important roles as the building blocks for external stimuli-responsive materials that are efficient energy converters and actuators. Here, we have developed a new hygromorphic metal oxide film capable of actuation, which is moved by fluid imbibition within a nano-capillary forest. This hygromorphic system is distinct from most of the reported hygromorphic actuating mechanisms such as the swelling of polymers by water, and multi- or bilayer platforms.[3,4,7] The actuating nano-capillary forest structure described here is made of superhydrophilic titanium oxide, and motion is triggered by water flow to produce structural transformation. The research results below suggest that this actuating nanostructure can improve humidity-responsive polymer actuators, high-efficiency energy converters and other applications.

MATERIALS AND METHODS

Synthesis of titanium oxide nano-capillary forest

Potentiostatic anodization of 0.25-mm-thick Ti foils (Nilaco, 99.99% purity) was performed at 60 V and 25 °C for 3 h in an ethylene glycol electrolyte (Sigma-Aldrich, 293237) containing 0.4 wt% NH_4F (Sigma-Aldrich, 216011) and 1 wt% deionized water using a platinum cathode (Nilaco, 99.99% purity). Before termination of anodization, the voltage was immediately decreased from 60 to 0 V within 1 s. After electrochemical etching, the nano-capillary forest was rinsed several times with ethanol and deionized water. After this rinsing, nitrogen was gently blown over the nano-capillary forest film. The large layer of cylindrical nano-capillary forest film having flexure was naturally detached during the gentle blowing procedure. Afterwards, it was kept in the vacuum desiccator for enough time (at least a day) before the experiment to completely dry and avoid chemical deposition on the film. Despite the possibility of residue forming inside the nano-capillary forest, the film was completely dried in the vacuum environment due to the high vapor pressure of the nano-sized water interface. The titanium oxide nano-capillary forest (TNF) was used immediately after complete drying.

[1]School of Mechanical Engineering, Sungkyunkwan University, Gyeonggi-do, Republic of Korea; [2]Department of Nature-Inspired Nanoconvergence Systems, Korea Institute of Machinery and Materials, Daejeon, Republic of Korea and [3]Department of Mechanical and Aerospace Engineering, Princeton University, Princeton, New Jersey, USA
Correspondence: Professor J Lee, School of Mechanical Engineering, Sungkyunkwan University, 2066 Seobu-ro, Jangan-gu, Suwon, Gyeonggi-do 16419, Republic of Korea.
E-mail: lee.jinkee@skku.edu
Received 12 January 2017; revised 16 May 2017; accepted 22 May 2017

Water-reactive actuation

One edge of a free-standing film was fixed between two glass slides covered with hydrophobic tape. Then, we placed a 5 μl drop of deionized water onto the film using a syringe. The water evaporated naturally under atmospheric conditions. The actuation angle of the film for each cycle was observed using an optical charge-coupled device (CCD) camera (Manta, MG 282C IRC). To demonstrate the energy density of a free-standing metal oxide film, we measured the generated mechanical force of a TNF film using a piezoelectric load cell (Ohaus, EX224G) after a 5 μl drop of deionized water was placed onto the dried free-standing film.

ESEM measurement method

We have documented capillary imbibition on the TNF structure using an environmental scanning electron microscope (ESEM, Quanta, FEG-250). The samples were mounted on a Peltier cooled specimen holder using double-sided copper tape for high heat conduction. The chamber pressure condition for condensation is over 700 Pa. Once the pressure is below 745 Pa, water condensed on the Peltier substrate and imbibed into nano-capillary gaps.

Energy-dispersive X-ray spectroscopy and X-ray diffraction results for TNF for analysis of the crystal structure

The energy-dispersive X-ray spectroscopy (EDX, Oxford, X-Max) and X-ray diffraction (XRD, Bruker, D8 discover) results show that the electrochemically produced free-standing nano-forest film (TNF) consists of the anatase crystal structure titanium oxide (Supplementary Figure S2). EDX was conducted for 60 s to obtain high accuracy. XRD scans were performed every 1 rotating degree from 0 to 90°.

Tensile and bending stress measurements

We measured the tensile and bending stresses using a tensile compression tester (Instron, model 3343) with a 5 N load cell to characterize the elasticity of the TNF film. The tensile modulus was measured by pulling the TNF film after gripping both ends. The three-point bending test was conducted to measure the bending stress of the TNF film. Because the TNF film has different top and bottom surface characteristics, we measured its bending stress in two different directions (on the top and bottom surfaces).

RESULTS AND DISCUSSION

A free-standing film of titanium oxide with an anatase crystal structure (Figure 1) and a high aspect ratio (length/radius ~80) has been developed in the form of nano-capillaries that are produced using electrochemical methods. The fabrication procedure is described in the experimental section and Supplementary Figure S1. EDX and XRD results confirmed the composition and crystal structures (Supplementary Figure S2). The fabricated free-standing film is curved (Figure 1a). The closed-end cylindrical nano-forest structure, including the side, top, and bottom, are analyzed using scanning electron microscopy (SEM); Figures 1b–d. The capillaries are well aligned with an 8-μm length (Figure 1b) on average, and the gaps between capillaries are ~5–20 nm. As shown in Figure 1c, the top side of the film has an open geometry, and the average inner and outer diameters are ~100 and 135 nm, respectively. Between the capillaries, there are gaps where water can flow through the film. The bottom side of the films, which is shown in Figure 1d, has closed-end caps, and the average outer diameter is 158 nm, with gaps between capillaries similar to those on the top. The gaps along the top side are wider than those at the bottom. This curved nano-forest has a superhydrophilic property with a contact angle of less than 3° (Supplementary Figure S3).

A schematic of the flow phenomenon within the titanium oxide nano-capillary forest (TNF) film as water flows through the gaps between the capillaries is shown in Figure 2a. Water flows from one side to another through gaps between closed-end capillaries, as shown by the red arrow. The 5–20 nm gaps between capillaries imbibe water by a strong Laplace pressure.[16] Obviously, water imbibes into closed-end capillaries but cannot flow through, as shown by the blue circle.[17] We have documented this water transport using an environmental scanning electron microscope (ESEM, Quanta, FEG-250). The chamber pressure conditions for dry and wet surfaces are, respectively, below 700 Pa (Figures 2b and c) and over 745 Pa (Figures 2d and e). Once the pressure reaches 745 Pa, water condenses on the top surface of the TNF, as shown in Figure 2d. This water flow through the film is observed at the bottom side in Figure 2e and clearly shows that the nanometer-sized open gaps (red circles of Figure 2c) were filled with water since the black voids disappeared in Figure 2e under wet conditions. Additionally, the partially imbibed water in the closed-end capillary does not change the diameter of the titanium oxide tube, as shown in Figures 2b and d. Thus, we can presume that this partial imbibition does not alter the actuation. These ESEM experimental results are a significant clue for understanding the mechanism for our synthetic TNF actuator.

The mechanism leading to the reversible bending and unbending of the TNFs relies on the interplay of the interfacial force and the van der Waals force when the material is hydrated or dried. These forces play an important role in stabilizing the TNF's form when it is actuated by water. If there is no water, the surface tension is zero, and the capillaries are stuck together by the van der Waals force. Using a scaling analysis, the competition between the interfacial force and the van der Waals force is analyzed. To simplify, the interaction between two capillaries is considered. The van der Waals force per unit width of two capillaries, F_v, is scaled as $F_v \approx AL_c\sqrt{r}/16\sqrt{d^5}$, where A is the Hamaker coefficient ($\sim 10^{-19}$ N m), L_c and r are, respectively, the length and radius of the titanium oxide capillaries, and d is the average gap between the capillaries. The capillary force per unit gap between capillaries, F_w, is scaled as $F_w \approx \gamma L_c r\cos\theta/d$, where γ is the water surface tension coefficient between liquid and air and θ is the contact angle of the liquid with the titanium oxide tube surface (~3°). The force ratio (F_w/F_v) is higher than $\sim 10^3$. This large enough force ratio confirms that the interfacial force is the dominant force for actuation. The capillary size is dominantly affected by imbibition rather than by surface tension and contact angle variation, with a minor influence during hydration because F_v is still very small even if F_w varies by surface tension and contact angle. When water is completely dried, $F_w = 0$ due to the absence of an air-water meniscus and the van der Waals force acts to return the TNF to its initial shape.

Many cycles of actuation were observed by repeating experiments under controlled temperature and humidity. A TNF, 10 mm wide and 60 mm long, was placed in a high-precision environmental control unit (Daeyang, TH-180S) at 25 °C and 40% relative humidity. One edge of the free-standing film was fixed between two micro glass slides covered with a hydrophobic tape, and then a 5 μl water drop was placed on the TNF. The time-dependent deformations of the free-standing film were analyzed using optical image correlation (Figure 3a and Supplementary Movie 1). The measured angle versus time and its reproducibility are shown in Figure 3b and the inset, respectively. The sequential addition of water drops, which subsequently evaporate, show a repeating bending/unbending response without any fatigue. We made multiple TNF films, and all of them actuated, although the actuating angle varies depending on factors such as the length of the nano-capillary, the length of TNF film and the initial curvature of the TNF film.

The inhomogeneous initial gap on the top and bottom of TNF between the tubes due to the flexure of the film gives one of the key mechanisms of actuation. The actuation mechanism can be divided

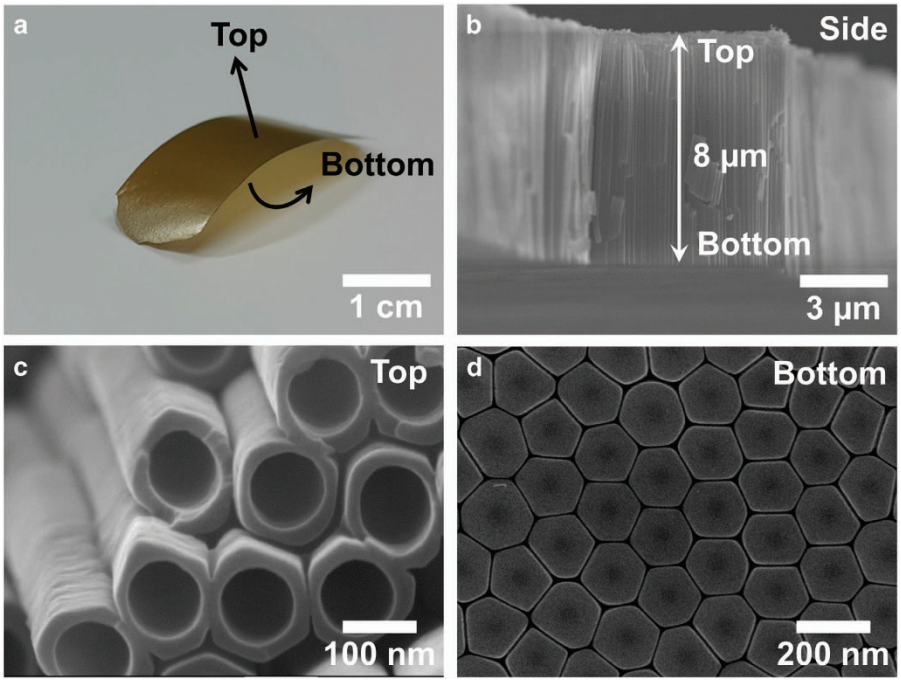

Figure 1 Optical and SEM images of the TNF free-standing film. (**a**) An optical image of a detached free-standing film. (**b**–**d**) SEM images of the (**b**) side, (**c**) top, and (**d**) bottom of a dried TNF film. The cylindrical nano-capillary forest was linearly well aligned with an average length of ~8 μm. The bottom side of the film has a cap, and the gap between the capillaries is ~5–20 nm. The top side of the film has open-ended capillaries with an average inner diameter of ~100 nm.

into four steps. First, when a drop of water is applied on the surface of TNF, the water penetrates through the film instantaneously by strong capillary force between gaps. The titanium oxide nano-capillaries are pulled together by interplay of the capillary force and the van der Waals force while water spreads along the TNF surface and imbibes through it until the deflection angle from the vertical reaches ~55° (Figure 3c—step I). For example, when a drop of water is applied on an impermeable surface of low contact angle, the water is expected to spread approximately according to Tanner's law of $R(t) \sim t^{0.1}$, where R is the radius and t is the time.[18] In this research, since the nano-capillaries are stabilized by the van der Waals force and the film is permeable, the directional spreading in the width direction and along the length is faster, $R(t) \sim t^{0.5}$ (reminiscent of Washburn's law (Supplementary Figure S4)). From the bending motion, the timescale for the first deformation regime is approximately 10 s. We believe that this timescale is set due to the slow spreading over the surface through the porous film following Washburn's law. In addition, as water spreads on the surface, it rapidly imbibes through 5–20 nm gaps of the films.[19] It follows that the pressure of imbibed water (P_{water}) is lower than atmospheric pressure (P_{atm}) since the surface of TNF is super-hydrophilic. Once water imbibes through the film, the capillary-produced pressure difference, or internal stress distribution, pulls the outer surface of each capillary to produce bending. When water has fully filled in the gaps between the capillaries, the free-standing TNF film remains unbent for ~2 min (Figure 3d—step II). Then, as evaporation of water proceeds, the film bends more to ~100° (Figure 3e—step III). As shown in Figure 3b, the response speed of step III of actuation is slower than that of step I since the water evaporation rate is slower than the rate of water spreading and imbibition. In the case of dehydration, the drying direction by flexure of film is important with the narrow gaps drying earlier due to high vapor pressure by meniscus. This makes the actuator move even forward. When water fully evaporates, the van der Waals force alone acts on the capillaries, and the TNF film returns to its initial state (step IV). During actuation, the asymmetrical width-directional spreading and drying of water on the TNF film cause out-of-plane twisting motion.

To demonstrate a potential application of actuation of the free-standing film, we estimated the mechanical energy as an energy-collecting cantilever system. When the steps of water imbibition and evaporation are repeated, the free-standing film bending and unbending cause a mechanical force, as shown in Figure 4a. During an actuation cycle, the generated force varies and reaches a maximum of 0.62 mN as measured by a load cell (Ohaus, EX224G). In fact, only ~15 mg of the titanium oxide nano-capillary films generated a larger force than most other actuating devices on a per mass basis.[20–24]

Because the strain energy varies throughout a body, it is convenient to use the concept of strain energy density, which is a measure of how much energy is stored in small-volume elements throughout a material. To calculate the energy density of the free-standing TNF film, we assumed that the film is a uniform geometry in the form of an end-loaded cantilever of length L and calculated the strain energy for normal stresses acting in the elastic material upon deformation by a steadily increasing force F. The work done in extending the cantilever by a small amount, dx, is stored as elastic strain energy U, given as $U = F\mathrm{d}x$. In the case of linear elastic deformation for a cantilever subjected to a bending load, the stress is $\sigma_x = My/I$, where M is the moment, I is the area moment of inertia and volume is $\mathrm{d}V = \mathrm{d}A\mathrm{d}x$. Then, the elastic strain energy $U = \int \sigma_x^2/2E \ \mathrm{d}V = \int_0^L M^2/EI \ \mathrm{d}x$, where E is Young's modulus. For an end-loaded cantilever, $U = \int_0^L F^2x^2/2EI \ \mathrm{d}x = F^2L^3/6EI$, since $M = -Fx$. The Young's modulus of the TNF film is directly measured as 700 ± 126 MPa (Supplementary Figure S5, Instron, model 3343). Since bulk TiO_2 has a very large Young's modulus of ~230–280 GPa, the low tensile Young's modulus value provides evidence of its elasticity coming from the gaps between capillaries. For bending stress, we measured in two

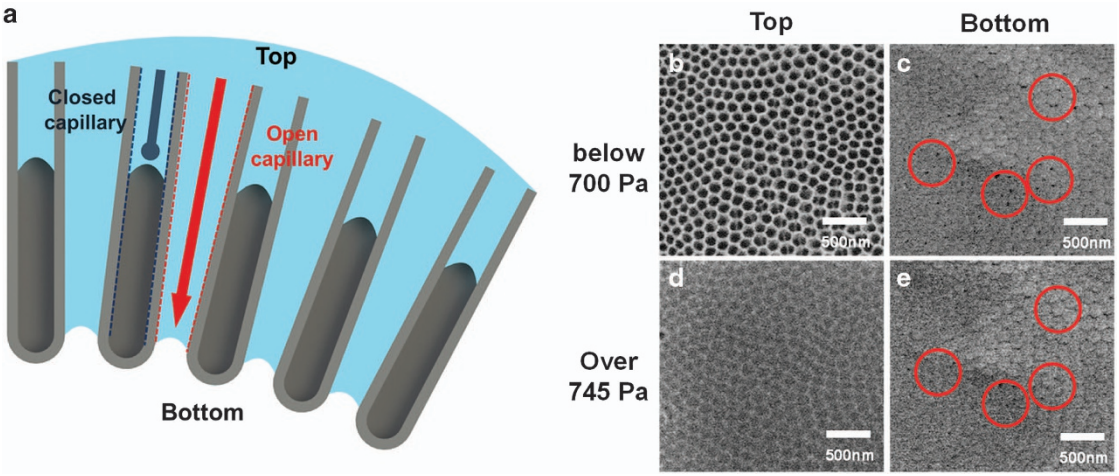

Figure 2 Water penetration through the TNF capillaries. (**a**) Schematic of TNF structure and water penetration path (**b**–**e**). Environmental scanning electron microscopy (ESEM) images of the top (**b**, **d**) and bottom (**c**, **e**) side of TNF as a function of humidity conditions. When the ESEM chamber pressure is below 700 Pa, it is considered a dry condition, whereas a chamber pressure over 745 Pa corresponds to a wet condition. The red circles show voids (**c**) and water-filled gaps (**e**).

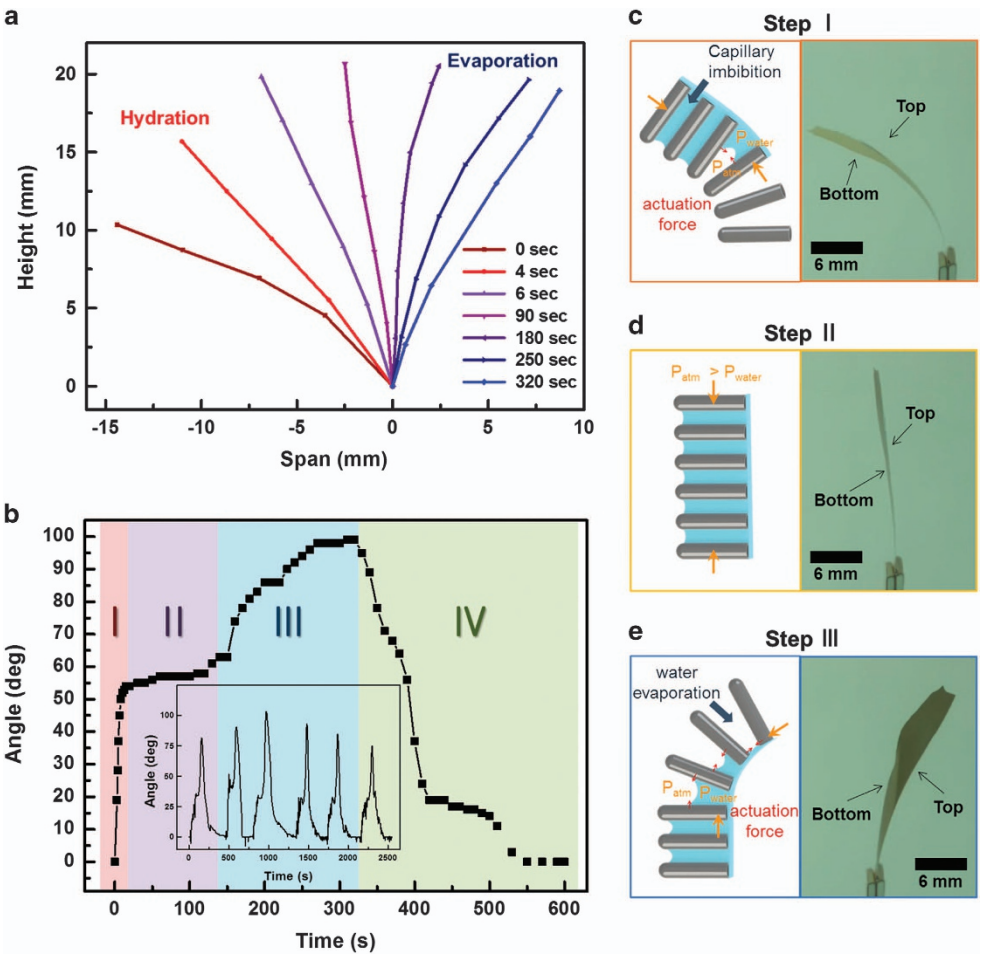

Figure 3 Hygromorphic actuating motion of the TNF free-standing film. (**a**) The stepwise changes in the free-standing film by tracking progressive movements. (**b**) The bending angle of the free-standing film versus time after water is placed on the film and then dried. The initial position was chosen to be the zero angle reference. The inset shows the repeatability of the actuation over many cycles. (**c**–**e**) The schematics and optical images of each actuation step.

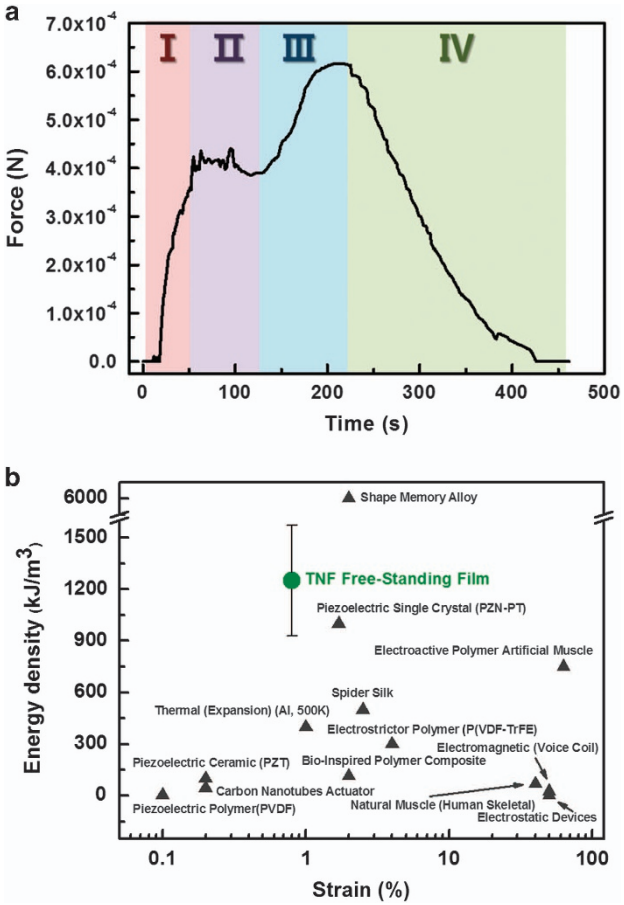

Figure 4 Mechanical force and energy density of the TNF free-standing film. (**a**) The measured mechanical force during an actuation cycle. The force reaches 0.62 mN at the end of step III. (**b**) Comparison of the results in the estimated energy densities and strain responses of the TNF film with typical values reported for materials frequently used or studied in the context of actuators and stimuli-responsive materials.

different directions since the TNF film has different top and bottom surface characteristics (Supplementary Figure S6). When the TNF film was forced on the top surface, as shown in Supplementary Figure S6b, it started to bend until fracture, with a maximum bending stress at 23.77 MPa. On the bottom surface (Supplementary Figure S6c), the maximum bending stress was found to be 8.25 MPa. Obviously, the different bending stress is attributed to the gap distance difference for both surfaces. The calculated average strain energy density (energy/volume) of the TNF film was remarkably high, $U/V \sim 1250 \pm 323$ kJ m^{-3}. Figure 4b compares the estimated energy densities and strain responses of the TNF film with typical values reported for materials frequently used or studied in the context of actuators and stimuli-responsive materials.[20–24] At this point, even though this TNF actuator has a much lower energy density than a shape memory alloy, it still shows a relatively high energy density compared to other actuators with sustainability and repeatability. Since this actuator uses a new hygromorphic actuating mechanism, it could be a useful actuator once the obstacles, such as response time and actuation speed, are solved.

CONCLUSION

In this paper, we have successfully fabricated a hygromorphic actuator from a titanium oxide nano-capillary forest film that has structural and compositional features capable of actuation. The TNF film actuates by water spreading on the surface with imbibition through it and subsequent evaporation. When water is imbibed through a film, the actuator starts to bend, and during evaporation, it moves forward and then returns to the original structure when the water completely evaporates. The actuating timescale is set due to the slow spreading over the surface through the porous film according to Washburn's law. The deformation is repeatable with a relatively high energy density of ~ 1250 kJ m^{-3}, and this nano-capillary forest has unique capabilities that may lead to novel stimuli-responsive systems, including energy collecting and storage as well as robotics applications.

CONFLICT OF INTEREST

The authors declare no conflict of interest.

ACKNOWLEDGEMENTS

We appreciate the support provided by the Basic Science Research Program through the National Research Foundation of Korea (NRF) funded by the Ministry of Science, ICT and Future Planning (2014M3C1B1033982 and 2017M3C1B7014239).

PUBLISHER'S NOTE

1 Stuart, M. A. C., Huck, W. T. S., Genzer, J., Muller, M., Ober, C., Stamm, M., Sukhorukov, G. B., Szleifer, I., Tsukruk, V. V., Urban, M., Winnik, F., Zauscher, S., Luzinov, I. & Minko, S. Emerging applications of stimuli-responsive polymer materials. *Nat. Mater.* **9**, 101–113 (2010).
2 Yu, Y., Maeda, T., Mamiya, J. I. & Ikeda, T. Photomechanical effects of ferroelectric liquid-crystalline elastomers containing azobenzene chromophores. *Angew. Chem.* **119**, 899–901 (2007).
3 Fukushima, T., Asaka, K., Kosaka, A. & Aida, T. Fully plastic actuator through layer-by-layer casting with ionic-liquid-based bucky gel. *Angew. Chem.* **117**, 2462–2465 (2005).
4 Yamada, M., Kondo, M., Miyasato, R., Naka, Y., Mamiya, J., Kinoshita, M., Shishido, A., Yu, Y. L., Barrett, C. J. & Ikeda, T. Photomobile polymer materials-various three-dimensional movements. *J. Mater. Chem.* **19**, 60–62 (2009).
5 Feinberg, A. W., Feigel, A., Shevkoplyas, S. S., Sheehy, S., Whitesides, G. M. & Parker, K. K. Muscular thin films for building actuators and powering devices. *Science* **317**, 1366–1370 (2007).
6 Camacho-Lopez, M., Finkelmann, H., Palffy-Muhoray, P. & Shelley, M. Fast liquid-crystal elastomer swims into the dark. *Nat. Mater.* **3**, 307–310 (2004).
7 Maeda, S., Hara, Y., Sakai, T., Yoshida, R. & Hashimoto, S. Self-walking gel. *Adv. Mater.* **19**, 3480 (2007).
8 Kopecek, J. Polymer chemistry—swell gels. *Nature* **417**, 388 (2002).
9 Yoshida, R., Uchida, K., Kaneko, Y., Sakai, K., Kikuchi, A., Sakurai, Y. & Okano, T. Comb-type grafted hydrogels with rapid de-swelling response to temperature-changes. *Nature* **374**, 240–242 (1995).
10 Ahir, S. V. & Terentjev, E. M. Photomechanical actuation in polymer-nanotube composites. *Nat. Mater.* **4**, 491–495 (2005).
11 Hu, Z. B., Zhang, X. M. & Li, Y. Synthesis and application of midulated polymer gels. *Science* **269**, 525–527 (1995).
12 Wong, W. S. Y., Li, M., Nisbet, D. R., Craig, V. S. J., Wang, Z. & Tricoli, A. Mimosa origami: a nanostructure-enabled directional self-organization regime of materials. *Sci. Adv.* **2** (2016).
13 Dawson, C., Vincent, J. F. V. & Rocca, A.-M. How pine cones open. *Nature* **390**, 668–668 (1997).
14 Elbaum, R., Zaltzman, L., Burgert, I. & Fratzl, P. The role of wheat awns in the seed dispersal unit. *Science* **316**, 884–886 (2007).
15 Harrington, M. J., Razghandi, K., Ditsch, F., Guiducci, L., Rueggeberg, M., Dunlop, J. W. C., Fratzl, P., Neinhuis, C. & Burgert, I. Origami-like unfolding of hydro-actuated ice plant seed capsules. *Nat. Commun.* **2**, 337 (2011).
16 Pascal, T. A., Goddard, W. A. & Jung, Y. Entropy and the driving force for the filling of carbon nanotubes with water. *Proc. Natl Acad. Sci.* **108**, 11794–11798 (2011).
17 Lim, H., Tripathi, A. & Lee, J. Dynamics of a capillary invasion in a closed-end capillary. *Langmuir* **30**, 9390–9396 (2014).
18 Tanner, L. H. The spreading of silicone oil drops on horizontal surfaces. *J. Phys. D: Appl. Phys.* **12**, 1473 (1979).
19 Dimitrov, D. I., Milchev, A. & Binder, K. Capillary Rise in Nanopores: Molecular Dynamics Evidence for the Lucas-Washburn Equation. *Phys. Rev. Lett.* **99**, 054501 (2007).

20 Zhang, Q. M., Bharti, V. & Zhao, X. Giant electrostriction and relaxor ferroelectric behavior in electron-irradiated poly(vinylidene fluoride-trifluoroethylene) copolymer. *Science* **280**, 2101–2104 (1998).
21 Park, S.-E. & Shrout, T. R. Ultrahigh strain and piezoelectric behavior in relaxor based ferroelectric single crystals. *J. Appl. Phys.* **82**, 1804–1811 (1997).
22 Aliev, A. E., Oh, J., Kozlov, M. E., Kuznetsov, A. A., Fang, S., Fonseca, A. F., Ovalle, R., Lima, M. D., Haque, M. H., Gartstein, Y. N., Zhang, M., Zakhidov, A. A. & Baughman, R. H. Giant-stroke, superelastic carbon nanotube aerogel muscles. *Science* **323**, 1575–1578 (2009).
23 Agnarsson, I., Dhinojwala, A., Sahni, V. & Blackledge, T. A. Spider silk as a novel high performance biomimetic muscle driven by humidity. *J. Exp. Biol.* **212**, 1990–1994 (2009).
24 Ma, M., Guo, L., Anderson, D. G. & Langer, R. Bio-inspired polymer composite actuator and generator driven by water gradients. *Science* **339**, 186–189 (2013).

Supplementary Information accompanies the paper on the NPG Asia Materials website (http://www.nature.com/am)